Curr Cardiovasc Imaging Rep (2011) 4:116–126
DOI 10.1007/s12410-011-9067-7

Modeling and Registration for Electrophysiology Procedures Based on Three-Dimensional Imaging

Kawal Rhode · Maxime Sermesant

Published online: 20 January 2011

Abstract Computer models of cardiac electrophysiology (EP) can help to better understand the mechanisms of arrhythmias and to guide interventions. However, model adjustment to patient data (personalization) is a required step that is still challenging from clinical data. The progress in the fusion of multimodal data opens up new possibilities in generating patient-specific models of the heart. In this paper, we present the state-of-the-art in multimodal data fusion for EP procedure guidance and how such integrated data can be used to personalize models and guide interventions.

Keywords Cardiac electrophysiology model · 3D imaging · Image registration · Data fusion · Model personalization

Introduction

Electrophysiology (EP) procedures can be highly effective, but the complexity of the electromechanical phenomena combined with the challenges of cardiac catheterization still hamper the success rate. There has been an important effort in the last years in image fusion in order to help guidance of such procedures. This is often based on multimodal image registration, allowing the display of information from from computer tomography (CT) or magnetic resonance imaging (MRI) as an overlay on top of real-time fluoroscopy. However, the planning of the intervention is still difficult. The translation of the important effort in cardiac electrophysiology modeling into the clinical environment could help such interventional planning. We present here how the latest developments in image fusion can be coupled with personalized models of the heart in order to improve planning and guidance of EP procedures.

The two exemplar applications presented here are cardiac resynchronization therapy (CRT) and radiofrequency (RF) ablation. In the two cases, the image registration shares similar techniques but the biophysical models used are different. No global biophysical model of cardiac electrophysiology is suitable for all the clinical applications. There is an important requirement to select the right model for a specific application. The model has to represent the important phenomena for this application, but any additional complexity makes the personalization harder and the computational cost higher.

Modeling of the human body at all scales has been an important research effort of the last decades; see for instance the Physiome project (http://www.physiome.org) and the Virtual Physiological Human (VPH) [1]. Within this community, cardiac models have been particularly developed, and mostly for the electrophysiology [2–8••, 9••] (and references therein). Detailed biophysical modeling of cardiac EP can help in understanding the pathophysiology and the generic mechanisms. However, for personalized planning and guidance, there is a need to adjust the parameters of these models in order to fit to specific patient clinical data. This is also a scientific challenge, which is now an important focus of the modeling community.

This has been enabled by the tremendous progress of the imaging of the heart, and the fusion of the different imaging modalities. We present in this article a review of the imaging as well as examples of biophysical model personalization for EP procedure guidance.

K. Rhode · M. Sermesant (✉)
Imaging Sciences & Biomedical Engineering,
King's College London,
St. Thomas' Hospital,
London, UK
e-mail: maxime.sermesant@inria.fr

K. Rhode
e-mail: kawal.rhode@kcl.ac.uk

M. Sermesant
INRIA, Asclepios team,
Sophia Antipolis, France

Imaging Cardiac Anatomy/Function and Data Fusion for EP Procedures

Anatomical Imaging and Segmentation

Anatomical imaging of the heart is possible with CT, MRI, ultrasound (echocardiography, echo), and rotational X-ray angiography (RXA). Each imaging modality has its relative advantages and disadvantages and all can be used for interventional guidance of cardiac EP procedures and subsequent biophysical modeling.

CT imaging is now widespread and modern scanners can acquire an ECG-gated image of the whole heart within a single breath-hold following the injection of iodinated contrast agent [10•]. The voxel resolution is high at 0.3 mm^3. There is excellent visualization of the endocardial cavities, good visualization of the ventricular myocardium and the valves [11, 12]. However, the visualization of the atrial myocardium remains a challenge but is just discernable using this modality. Imaging of the coronary circulation is well achieved for both arteries and veins after contrast agent injection. Concerns about radiation dose are counter-balanced by new acquisition techniques, such as *step-and-shoot*, that keep dose to a minimum while maintaining high image quality [13].

Cardiac MRI has seen significant development in the last 10 years [14]. The use of ECG-gated and respiratory-navigated techniques allows the acquisition of a single high-resolution whole-heart image in less than 10 minutes during free-breathing acquisition. This can be carried out after gadolinium-based contrast agent injection to achieve excellent visualization of the endocardial cavities. There is excellent visualization of the left ventricular myocardium, but the visualization of the right ventricular and atrial myocardium is challenging due to the limits of the voxel resolution that can be typically reconstructed to 1 mm^3. Imaging of the coronary arteries is well achieved and visualization of the coronary venous system is possible, especially after the administration of blood-pool imaging contrast agents such as Gd-BOPTA (Bracco Imaging SpA, Italy). Imaging of the valves is limited using MRI.

Echocardiography is the mainstay of cardiac imaging due to its low cost and ubiquitous availability. Recent advances in transducer technology allow for the acquisition of wide field-of-view three-dimensional heart images using both transthoracic (TTE) and transesophageal (TEE) probes [15]. Whole-heart images can be reconstructed using image-stitching or compounding methods [16•]. Excellent visualization is possible of all of the cardiac chambers, the great vessels, the left ventricular myocardium, and the valves. Imaging of the right ventricular myocardium is more challenging. The atrial myocardium can be imaged effectively using transesophageal probes. There is also the possibility to use catheter-based intracardiac echo (ICE) to achieve small field-of-view detailed imaging from within the heart.

Rotational X-ray angiography uses conventional C-arm technology to acquire multiple projection images during the injection of iodinated contrast agent into the target structure. The C-arm is rotated around the patient during a breath-hold and is covering a typical rotation of more than 200° in less than 10 s. Reconstruction techniques are then applied to obtain CT-like image data with a typical reconstructed voxel resolution of 0.4 mm^3. RXA has been extensively used for imaging of the left atrium for guidance of left atrial ablation procedures [17•]. The contrast injection can be either directly into the left atrium, with cardiac motion arrested using either adenosine injection or rapid pacing [18]. Recently, RXA has been also used to image the right ventricle to guide the ablation of the right ventricular outflow tract tachyarrhythmias [19•]. RXA only provides images of the endocardial cavities, with poor signal-to-noise ratio and significant cardiac motion blur. RXA has also been used for imaging of the coronary circulation, both arteries and veins.

For effective use for image-guided intervention and biophysical modeling, anatomical models must be generated from the cardiac image data. This can be achieved by segmentation of the image data and subsequent surface meshing or by both of these in a single step, ie, direct surface fitting to the image data. Segmentation should be robust, ie, have a low failure rate, and accurate. The gold standard for cardiac segmentation is manual, slice-by-slice segmentation by an expert. This will be robust and accurate but is very time-consuming and can take 4 h for a several-hundred slice data set. The use of fully automatic or semiautomatic methods is preferred as long as the robustness and accuracy are within the requirements for interventional guidance and modeling. Fully automatic whole-heart segmentation (all cardiac chambers, including the left ventricular myocardium, and the great vessels) has been reported using statistical shape models (SSMs, see [20] for a detailed review of SSMs and their use for segmentation) and atlas-based methods. These methods have been applied to both CT [21••] and MR [22–24] image data (Fig. 1) and more recently to 3D echo data [25]. Robustness and accuracy are best for CT data where image quality and consistency is high. Segmentation results for cardiac MR image data are slightly inferior and methods are restricted to particular acquisition protocols, eg, steady-state free precession (SSFP) 3D data. Echo data poses the greatest challenge due to low signal-to-noise and field-of-view problems. For all imaging modalities, fully automated segmentation techniques coupled to minor expert manual corrections give a significant timesaving when compared to manual segmentation. In all cases, the segmentation of the

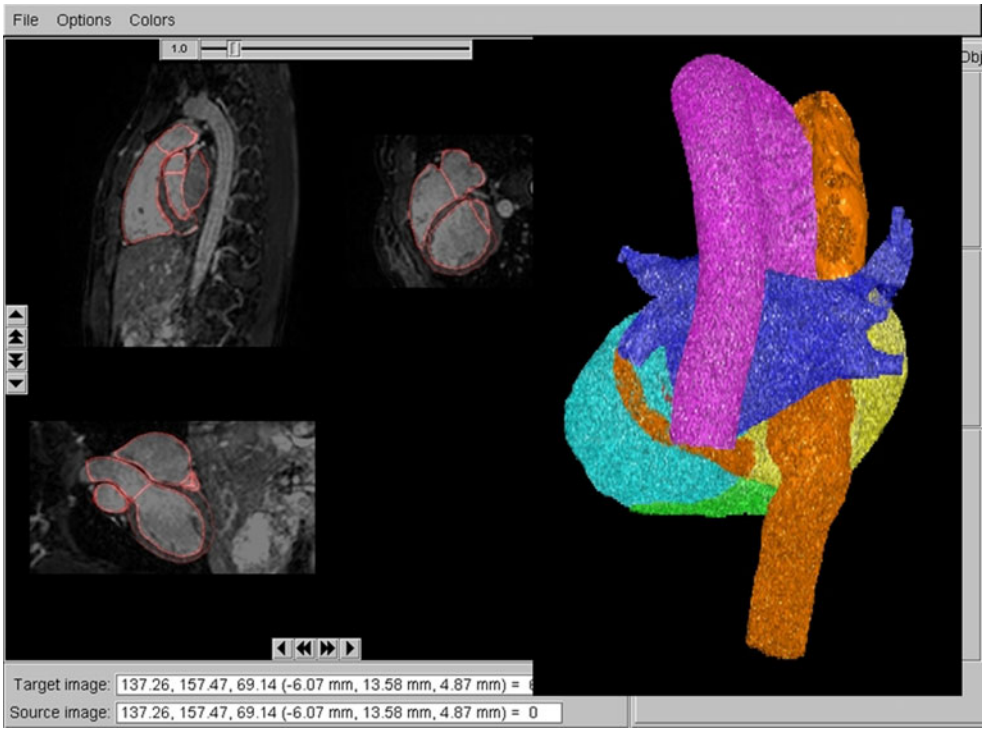

Fig. 1 Fully automatic segmentation result using the method of Peters et al. [22]. A high-resolution whole-heart SSFP MR dataset is shown in multiplanar view (*left*) with segmented boundaries shown in *red*. The resultant 3D model is shown on the *right* with the cardiac chambers and great vessels labelled with different colors: (*cyan*) left ventricle, (*green*) right ventricle, (*blue*) left atrium, (*yellow*) right atrium, (*brown top*) superior vena cava, (*brown bottom*) inferior vena cava, (*brown left*) coronary sinus, and (*magenta*) aorta

left atrial endocardium is a challenge due to the topological variants of the pulmonary veins that are present. Segmentation of the left atrium from RXA data using SSMs has been demonstrated but only for the four-vein pulmonary vein configuration [26]. Recent work on left atrial segmentation from first-pass gadolinium MR angiography image data [27] is promising but semiautomated techniques, such as ITK-Snap (http://www.itksnap.org) [28], are currently more robust for left atrial segmentation. Segmentation of the right ventricular or atrial myocardium remains a challenge and is largely limited by the current state-of-the-art in imaging. Segmentation of the valves has recently been demonstrated from cardiac CT data and also from echo data [11, 12].

Electro-anatomic mapping systems (EAMS) are extensively used during EP procedures for guidance and electrical mapping. These systems are able to reconstruct the geometry

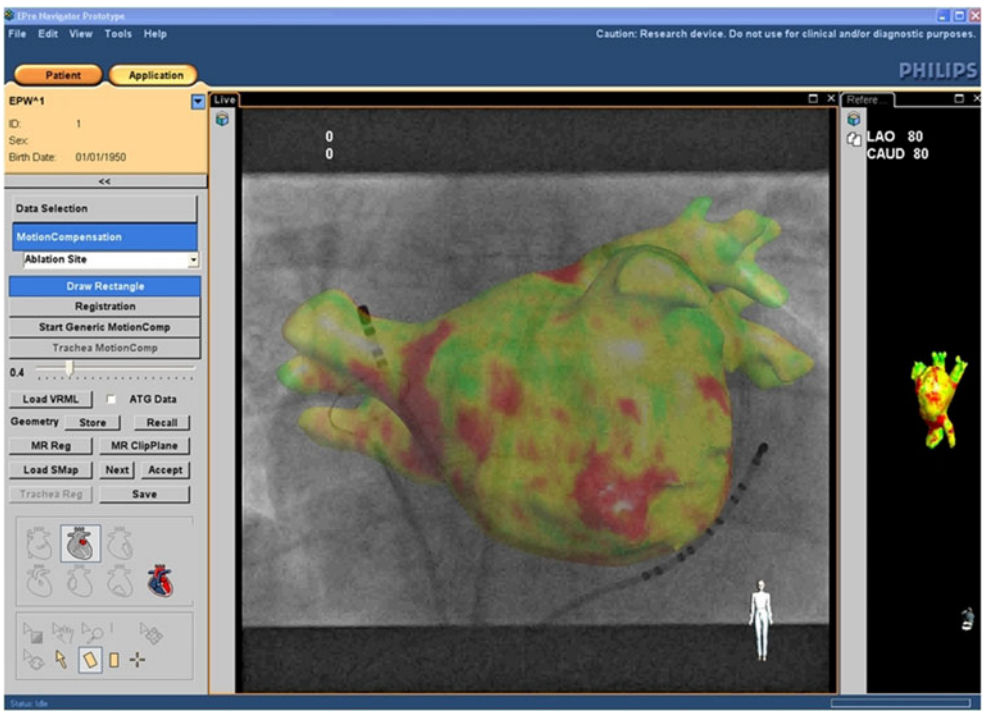

Fig. 2 Left atrial scar map registered to X-ray fluoroscopy to guide a redo left atrial ablation for atrial fibrillation. The anatomical surface and scar map were derived from MR SSFP and gadolinium late-enhancement images, respectively. The amount of late-enhancement is color-code with *red* as high, *green* as medium to low, and *yellow* as none. There is an ablation catheter (*middle catheter*) looped inside the left atrium and inserted into the right upper pulmonary vein. The *right catheter* is inside the coronary sinus and the *left catheter* is the lasso lying in the right atrium

of target cardiac chambers by tracking a roving catheter within the heart. As the roving catheter is moved along the endocardial surface, the position of the catheter is continually recorded to generate a surface model. Examples of these systems include the CARTO system (Biosense Webster, USA) [29••] and the EnSite NavX system (St. Jude Medical, USA) [30•]. Due to the limitations of the accuracy of the catheter tracking and the influences of both cardiac and respiratory motion, the fidelity of the anatomical reconstructions is suitable for the guidance of procedures but is of limited use for obtaining the high-fidelity anatomical models required for biophysical modeling.

Functional Imaging

Functional imaging can be divided into several categories: motion, perfusion/blood flow, and scar imaging. Motion imaging is possible with CT, MR, and echo imaging. Gated cardiac CT has an intrinsic temporal resolution of approximately 100 ms but image reconstruction is possible for any arbitrary cardiac phase, as expressed by the percentage of the R-R interval, using interpolation. Several techniques exist for imaging cardiac motion using MRI and the two most popular techniques are cine MRI and tagged MRI. Both cine and tagged MRI are typically acquired as a series of short-axis and long-axis slices, with 40 to 50 phases per slice for cine MRI and 20 to 30 phases per slice for tagged MRI [31•]. More recent advances in MRI have allowed whole-heart dynamic 3D imaging for both cine and tagged acquisitions but with lower temporal and spatial resolutions than the 2D counterparts [32]. However, 3D acquisitions do not have the inter-slice mis-registrations that are often present with the 2D acquisitions due to multiple breath-holds. Dynamic 3D imaging of the ventricles is possible with echo imaging with the latest transducers and systems achieving frame rates of 40 frames per second. See Leung and Bosch [33••] for a detailed review of techniques to extract the myocardial motion from this type of data.

MRI has been shown to be the premier modality for myocardial perfusion imaging and scar imaging [31•, 34]. Although perfusion imaging and scar imaging with CT is possible [35, 36], the sensitivity and robustness is poor when compared to MRI. Recently, gadolinium late-enhancement MRI has been used to image necrotic damage caused by catheter-based RF ablation for the treatment of atrial fibrillation and atrial flutter [37••, 38]. Post-processing techniques have been developed to segment and visualize these necrotic regions that resolve to form atrial scars over time (Fig. 2) [39••]. Furthermore, T2-weighted MRI has been used to image the acute edematous effects of RF ablation with some success [39••].

Electrical Mapping

For EP procedures, measurement and localization of the electrical activity of the heart is critical. Commercial

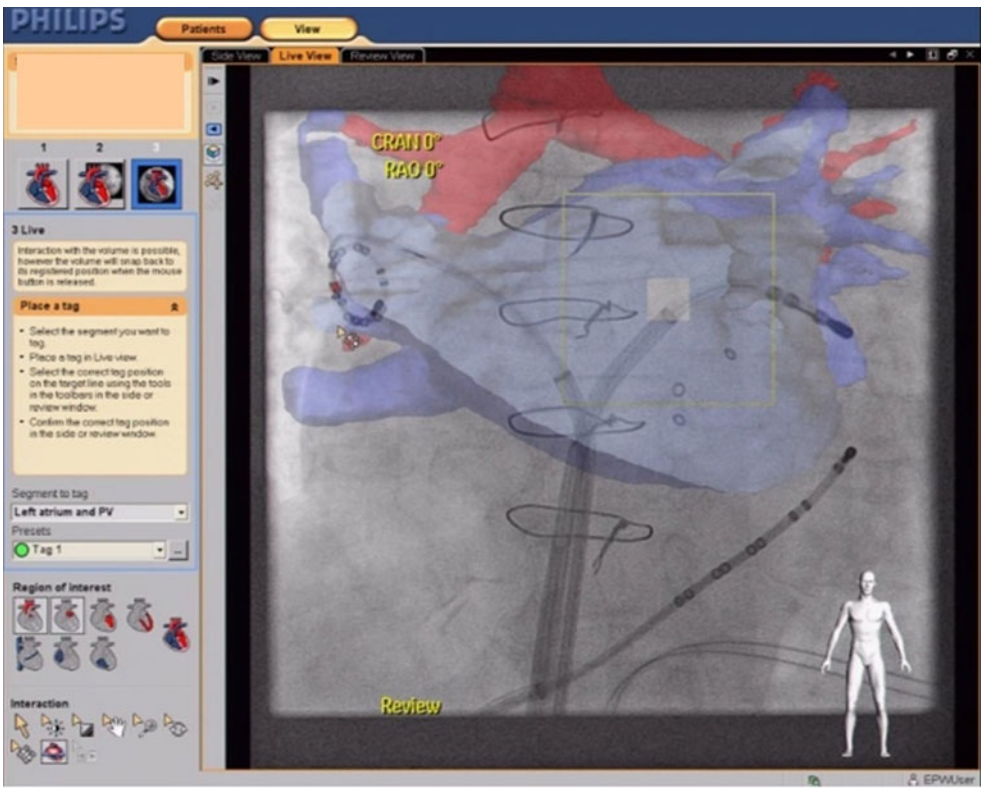

Fig. 3 Example of CT registration to X-ray fluoroscopy for guidance of ablation treatment of left atrial fibrillation. The left atrium is shown in a cut-away view in *blue*; the *red* structure is the tracheal bifurcation and this was used to aid in the manual registration of the CT data to the fluoroscopy data. Catheters can be seen inside the left atrium (*top*) and inside the coronary sinus (*bottom*)

EAMSs have the capability to record and localize the electrical activity measured by tracked mapping catheters and to display this on the reconstructed anatomical models that are created by these systems. Furthermore, it is possible to directly map the electrical data to anatomical surfaces obtained from high-quality imaging modalities such as CT, MRI, and RXA. The high-fidelity surface models obtained from these modalities can be registered to the reconstructed EAMS models using a combination of point-based and surface-based registration techniques (CARTO-Merge, Biosense Webster, USA [40]; EnSite Nav-X Fusion, St. Jude Medical, USA [41]). Electrical mapping is also possible by measuring the position of the mapping catheter using X-ray fluoroscopy and projecting this to a registered anatomical model (ElectroNav, Philips Healthcare, The Netherlands) [42•, 43].

Multimodal Data Fusion

For both guidance of cardiac EP procedures and personalization of biophysical models, it is necessary to co-register or fuse multimodal data from imaging modalities and catheter-based information, such as the location of ablation points, pacing sites, and electrical data. If an EAMS is used, then this can be achieved by using CARTO-Merge or EnSite NavX Fusion technology as described above. Other approaches consist of registration of the 3D imaging data to

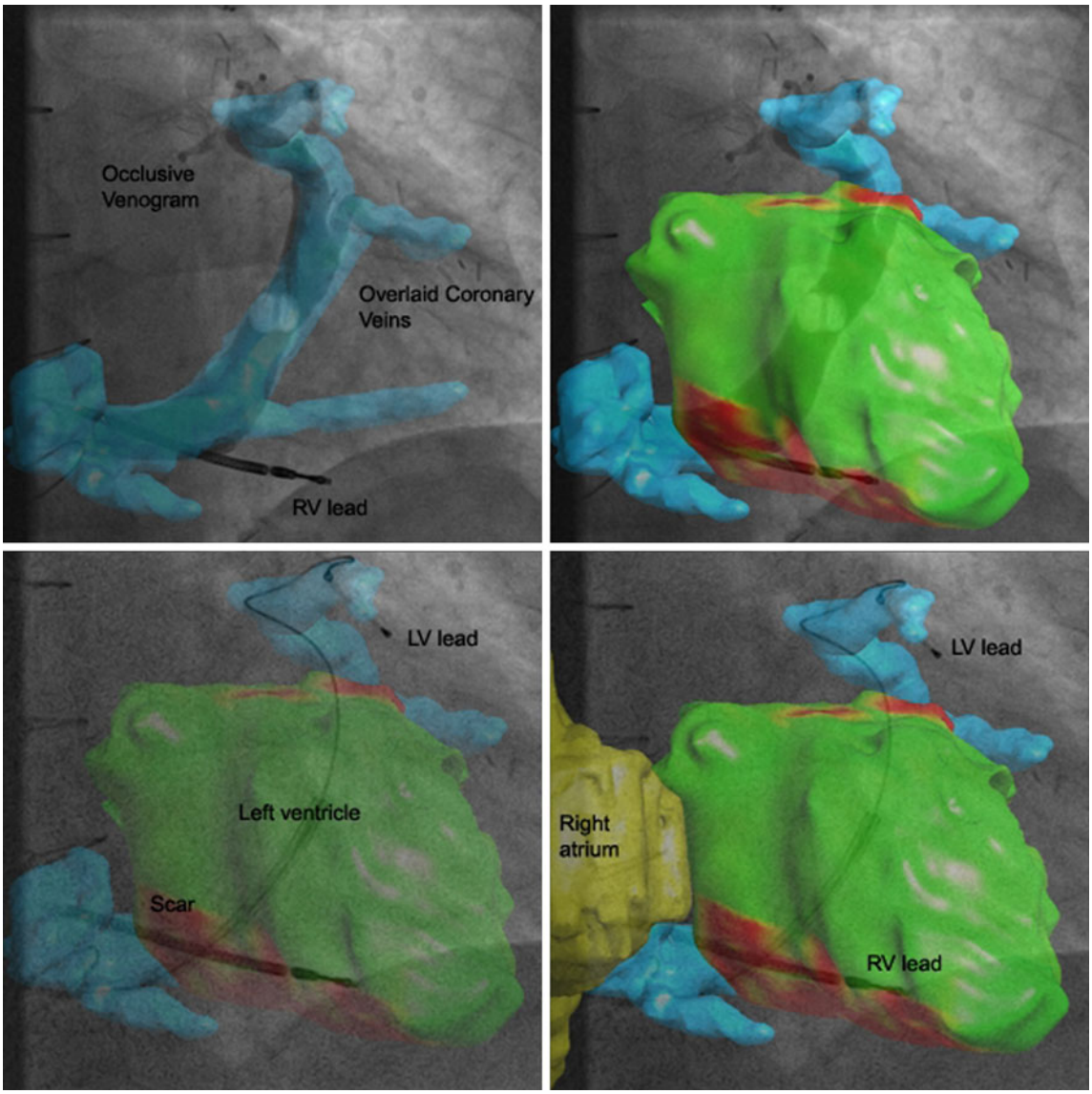

Fig. 4 Registration of MRI-derived data to X-ray fluoroscopy for the guidance of cardiac resynchronization therapy for the treatment of heart failure. The coronary venous system is shown in *blue*, the left ventricular endocardial surface is shown in *green* with scar distribution shown in *red*, and the left atrium is shown in *orange*, and the right atrium is shown in *yellow*. The balloon occlusive venogram (*top*) shows good alignment with the coronary vein model. In the shown position (*bottom*), the left ventricular lead is close to an area of scar

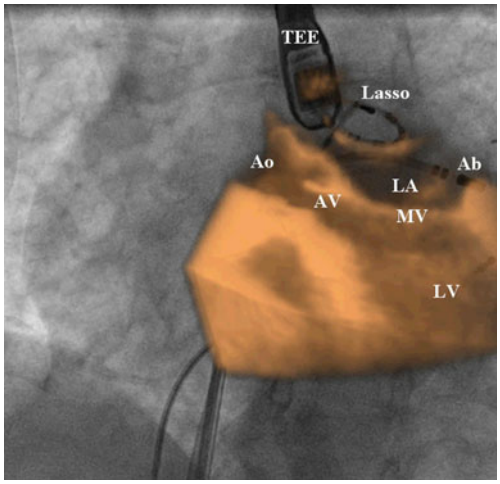

Fig. 5 Registration of 3D echo data (*orange*) to X-ray fluoroscopy (*grey scale*) by tracking a calibrated 3D transesophageal echo probe during left atrial ablation for the treatment of atrial fibrillationof atrial fibrillation. *TEE* - transesophageal echo probe, *Ao* - aorta, *LV* - left ventricle, *LA* - left atrium, *AV* - aortic valve, *MV* - mitral valve, *Lasso* - lasso catheter, *Ab* - ablation catheter

the 2D fluoroscopy images that are routinely used to guide EP procedures and to make catheter-based measurements. This problem is a 2D-3D registration problem (see [44•] for a detailed review of 2D-3D registration techniques for interventional guidance) but is somewhat challenging in the case of cardiac structures since there is limited common information available between the 3D and 2D image data. For the case of RXA data, the 2D-3D registration is implicit since both imaging data are acquired with the same X-ray system and therefore in the same coordinate system [45]. For CT and MR data, the registration can be performed in a number of ways. Manual alignment of CT-derived or MR-derived surface models with features seen in the fluoroscopy data (Figs. 2, 3, and 4), such as catheters, the heart borders, and contrast in angiography, can lead to a robust and accurate registration for guidance [46, 47]. This technology is available through the commercial EP Navigator platform (Philips Healthcare, The Netherlands). Automatic registration methods include the use of the spine [46] and 3D catheter reconstructions from multiple X-ray views [48, 49]. Automatic registration can also be achieved in the setting of hybrid X-ray/MR systems (XMR systems) by pre-calibration and tracking [50, 51••]. The registration of 3D echo data to fluoroscopy data is more challenging than when using 3D CT or MR data. Two approaches are possible: firstly, indirect registration via a registered CT or MR dataset [52, 53] or direct registration via a tracked echo probe (Fig. 5) [54, 55].

Modeling the Heart for EP Procedures

Biophysical Models of Cardiac Electrophysiology

For the last decades, an important research effort has focused on mathematical modeling of cardiac electrophysiology [4, 9••, 56••, 57, 58]. This effort has produced a

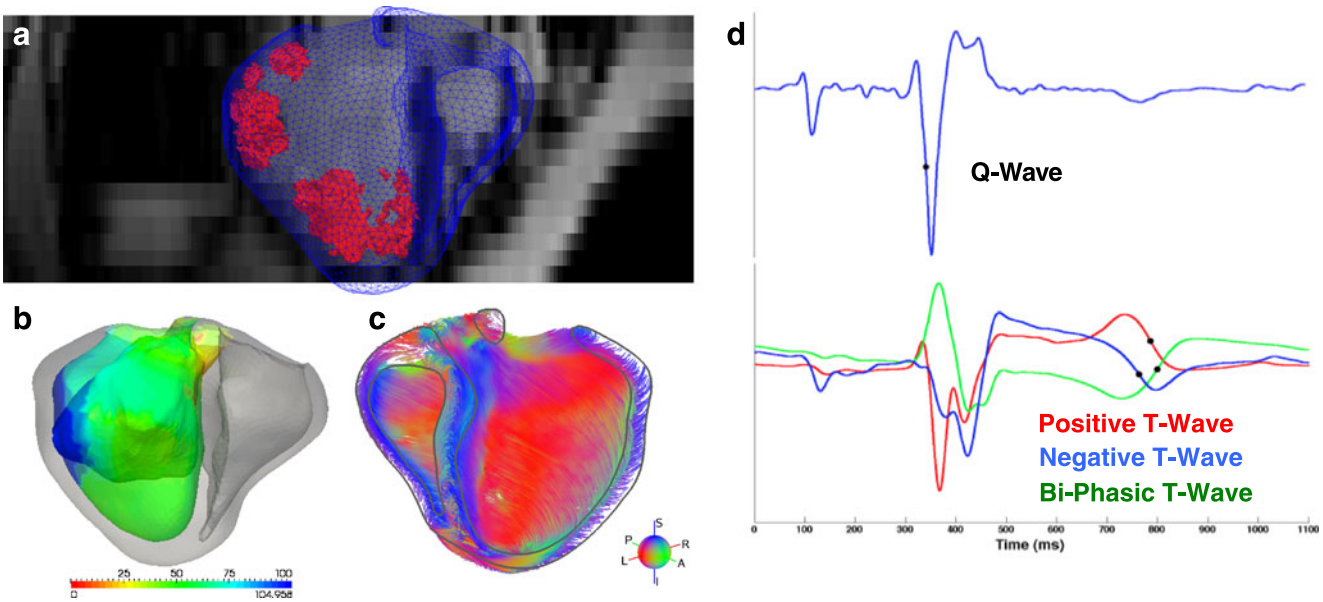

Fig. 6 From clinical data to models: **a** MR-derived segmented mesh with scars (*in red*); **b** XMR registration of Ensite LV surface with MR-derived mesh, values projected from Ensite to MR LV surface; **c** fiber orientations based on a statistical atlas; **d** unipolar electrograms for detection (*black dots*) of depolarization time (*upper*) and repolarization time (*lower*) from positive (*red*), negative (*blue*), and biphasic (*green*) T waves

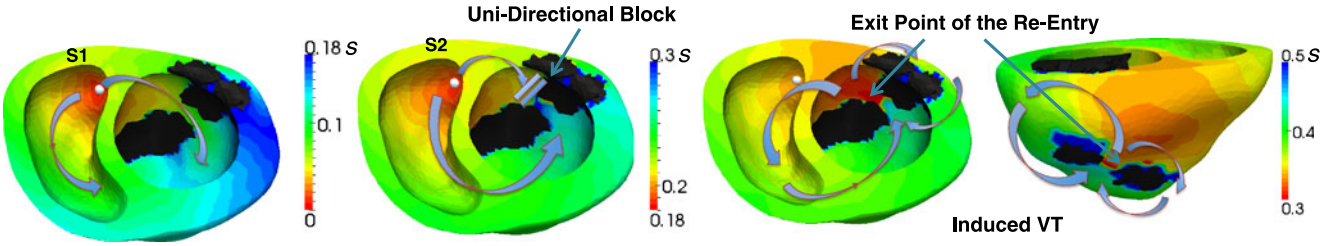

Fig. 7 DT isochrones for simulated S1-S2 VT-Stim protocol. S1 stimulus shows a normal propagation and S2 shows a unidirectional block created in the isthmus due to APD heterogeneity. Then we observe DT isochrones for induced monomorphic VT

variety of models, with different levels of complexity. An important question when translating such research into clinical applications is the choice of the relevant model. Indeed, the most complex models, which can reproduce the cardiac function with the most detailed realism, may not be the best choice as the complexity in adjusting the parameters and the computational time may not be compatible with the clinical constraints [59•, 60]. Computational modeling of cardiac arrhythmogenesis and arrhythmia maintenance using such models has made a significant contribution to the understanding of the underlying mechanisms [61–64]. These studies have shown a host of factors involved in the onset of arrhythmia with wave fragmentation and spiral wave breakups, which include realistic ventricular geometry [65], heterogeneity in repolarization [66], APD restitution [67, 68], and CV restitution [69]. A combined clinical study and synthetic modeling of APD restitution was shown [70], and comparisons with animal models were done for CRT [71, 72].

However, direct coupling of such models with clinical data to obtain patient-specific simulations and predictions remains challenging. Personalization of models, which is the process of estimating the model parameters that best fit a specific patient data, is now in important development [73, 74•]. It is a scientific challenge as modeling soft tissue in vivo is difficult and clinical data are usually sparse and noisy. Specific methods have to be designed, and these have to be fast and robust in order to be compatible with clinical constraints.

We present here an example of adjusting different parts of the model (geometry, conductivity, restitution) to the available clinical data (Fig. 6).

Anatomical Model Personalization

Biophysical models require first defining the spatial domain on which the simulations will be carried out. In the case of EP, one needs to segment the anatomical structure of interest (the atria or the ventricles). Different segmentation approaches, depending on the imaging modality, were presented in the first section.

It is then necessary to generate a computational mesh from the segmentation whose specifications are imposed by the equations of the model. The accuracy of the simulations is controlled by the characteristics of the mesh used.

Finally, one important factor of EP simulation is the muscle fiber orientation, as it has an impact on the action potential propagation. One can use synthetic orientations generated from the literature, or a statistical atlas built from ex vivo hearts [75], and potentially newly emerging in vivo measurements [76].

Electrophysiology Model Personalization

Adjusting the model parameters so that the simulation results fit the measured data is both a theoretical and practical challenge. This inverse problem can be ill posed; for instance, the solution may not be unique. This can be created by the only partial observation of the heart that is available. For instance, having only activation times on a part of the endocardium could lead to different volumetric parameters providing the same results. Thus it is important to evaluate the observability of the model parameters from the data, which provides insights on such topics.

This is the reason why the careful choice of the model is crucial for such methods, as more complex models may lead to situations where too many parameters are not

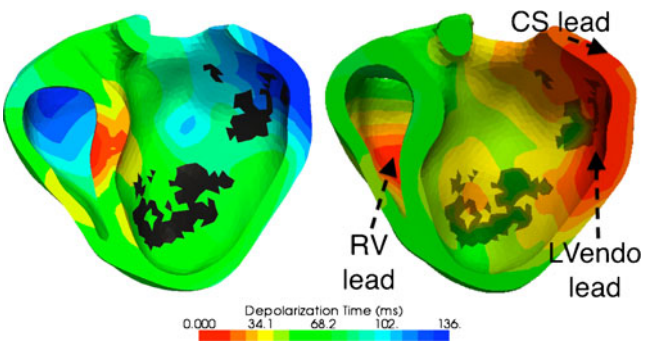

Fig. 8 Depolarization time isochrones estimated from the personalized electrophysiology model and the endocardial mapping data. Presented cases are sinus rhythm (*left*), and with pacing (*right*)

observable from the data, and thus its appropriateness to simulate patient-specific behavior is reduced.

Personalized Model Predictions

Once adjusted to the available patient data, models can be used to test the behavior of the heart under different conditions. We demonstrate here two examples, for VT and for CRT.

For instance, the VT stimulation procedure can be applied virtually to the model, in order to evaluate the inducibility of VT in the patient [77]. Once personalized using mapping data, different pacing protocols can be tested on the computer model, from any location in the heart (Fig. 7).

Similarly, personalized models of the heart were used to predict the changes in left ventricular pressure with different pacing conditions [78]. Personalized EP models were used to extrapolate the endocardial mapping data to the whole myocardium (Fig. 8), in order to then simulate contraction.

Conclusions

The important progress achieved in image acquisition, image fusion, and biophysical modeling opens up possibilities in obtaining patient-specific models of the heart. However, there is still an important challenge in order to perform this in a fast and robust manner, which is a required step before being able to use such models in a clinical environment. Moreover, the validation of model predictions on a large cohort of patients is still to be done. Once validated, such personalized models will be able to help in diagnosis and therapy planning.

Disclosure No potential conflicts of interest relevant to this article were reported.

References

Papers of particular interest, published recently, have been highlighted as:
- • Of importance,
- •• Of major importance

1. N. Ayache, J.-P. Boissel, S. Brunak, G. Clapworthy, G. Lonsdale, J. Fingberg, A. Frangi, G. Deco, P. Hunter, P. Nielsen, M. Halstead, R. Hose, I. Magnin, F. Martin-Sanchez, P. Sloot, J. Kaandorp, A. Hoekstra, S. Van Sint Jan, and M. Viceconti, "Towards virtual physiological human: Multilevel modelling and simulation of the human anatomy and physiology," Virtual Physiological Human: White paper, EC - DG INFSO and DG JRC, 2006.
2. A. McCulloch, J. Bassingthwaighte, P. Hunter, D. Noble, T. Blundell, and T. Pawson, "Computational biology of the heart: From structure to function." Progress in Biophysics & Molecular Biology, vol. 69, no. 2/3, pp. 151–559, 1998.
3. P. Hunter, A. Pullan, and B. Smaill, "Modeling total heart function," Annual Review of Biomedical Engineering, vol. 5, pp. 147–177, 2003.
4. D. Noble, "Modeling the heart," Physiology, vol. 19, pp. 191–197, 2004.
5. D. Nickerson, M. Nash, P. Nielsen, N. Smith, and P. Hunter, "Computational multiscale modeling in the IUPS physiome project: Modeling cardiac electromechanics," Systems Biology, vol. 50, no. 6, pp. 617–630, 2006.
6. E. J. Crampin, M. Halstead, P. Hunter, P. Nielsen, D. Noble, N. Smith, and M. Tawhai, "Computational physiology and the physiome project," Experimental Physiology, vol. 89, no. 1, pp. 1–26, Jan 2004.
7. P. Hunter and P. Nielsen, "A strategy for integrative computational physiology," Physiology (Bethesda), vol. 20, pp. 316–325, Oct 2005.
8. •• M. Fink, S. A. Niederer, E. M. Cherry, F. H. Fenton, J. T. Koivumki, G. Seemann, R. Thul, H. Zhang, F. B. Sachse, D. Beard, E. J. Crampin, and N. P. Smith, "Cardiac cell modelling: Observations from the heart of the cardiac physiome project," Progress in Biophysics and Molecular Biology, vol. In Press, 2010. *This is a recent review of the different cardiac cell models.*
9. •• R. Clayton, O. Bernus, E. Cherry, H. Dierckx, F. Fenton, L. Mirabella, A. Panfilov, F. Sachse, G. Seemann, and H. Zhang, "Models of cardiac tissue electrophysiology: Progress, challenges and open questions," Progress in Biophysics and Molecular Biology, vol. In Press, 2010. *This is a recent review of cardiac electrophysiology models.*
10. • Wijesekera NT, Duncan MK, Padley SP. X-ray computed tomography of the heart. Br Med Bull. 2010;93:49-67. *This summarizes the state-of-the-art for cardiac CT.*
11. Ionasec RI, Voigt I, Georgescu B, Wang Y, Houle H, Vega-Higuera F, Navab N, Comaniciu D. Patient-specific modeling and quantification of the aortic and mitral valves from 4-D cardiac CT and TEE. IEEE Trans Med Imaging. 2010 Sep;29(9):1636-51.
12. Waechter I, Kneser R, Korosoglou G, Peters J, Bakker NH, van der Boomen R, Weese J. Patient specific models for planning and guidance of minimally invasive aortic valve implantation. Med Image Comput Comput Assist Interv. 2010;13(Pt 1):526-33.
13. Efstathopoulos EP, Kelekis NL, Pantos I, Brountzos E, Argentos S, Grebác J, Ziaka D, Katritsis DG, Seimenis I. Reduction of the estimated radiation dose and associated patient risk with prospective ECG-gated 256-slice CT coronary angiography. Phys Med Biol. 2009 Sep 7;54(17):5209-22.
14. Stehning C, Boernert P, Nehrke K. Advances in coronary MRA from vessel wall to whole heart imaging. Magn Reson Med Sci. 2007;6(3):157-70.
15. Mor-Avi V, Sugeng L, Lang RM Real-time 3-dimensional echocardiography: an integral component of the routine echocardiographic examination in adult patients? Circulation 2009;119: 314-29.
16. • Yao C, Simpson JM, Schaeffter T, Penney GP. Spatial compounding of large numbers of multi-view 3D echocardiography images using feature consistency. 2010 7th IEEE International Symposium on Biomedical Imaging: From Nano to Macro, ISBI 2010 - Proceedings 2010, Article number 5490149, Pages 968-971. *This describes how multi 3D echo acquisitions can be used to overcome the field of view limitations with current transducer technology.*
17. • Orlov MV, Hoffmeister P, Chaudhry GM, Almasry I, Gijsbers GH, Swack T, Haffajee CI. Three-dimensional rotational angiography of the left atrium and esophagus–A virtual computed tomography scan in the electrophysiology lab? Heart Rhythm.

2007 Jan;4(1):37-43. *This article describes left atrial RXA imaging.*
18. Ector J, De Buck S, Nuyens D, Rossenbacker T, Huybrechts W, Gopal R, Maes F, Heidbüchel H. Adenosine-induced ventricular asystole or rapid ventricular pacing to enhance three-dimensional rotational imaging during cardiac ablation procedures. Europace. 2009 Jun;11(6):751-62.
19. • Orlov MV, Ansari MM, Akrivakis ST, Jadidi A, Nijhof N, Natan SR, Wylie JV, Hicks A, Armstrong J, Jais P. First Experience with Rotational Angiogram of the Right Ventricle to Guide VT Ablation. Heart Rhythm. 2010 Oct 1. *This article describes novel use of RXA for right ventricular imaging and also describes the ElectroNav electrical mapping system.*
20. • Heimann T, Meinzer HP. Statistical shape models for 3D medical image segmentation: a review. Med Image Anal. 2009 Aug;13 (4):543-63. *Reviews SSMs for use in segmentation and has an extensive coverage related to the heart.*
21. •• Ecabert O, Peters J, Schramm H, Lorenz C, von Berg J, Walker MJ, Vembar M, Olszewski ME, Subramanyan K, Lavi G, Weese J. Automatic model-based segmentation of the heart in CT images. IEEE Trans Med Imaging. 2008 Sep;27(9):1189-201. *Describes a robust, accurate, and fast method for whole-heart segmentation from CT data.*
22. Peters J, Ecabert O, Meyer C, Schramm H, Kneser R, Groth A, Weese J. Automatic whole heart segmentation in static magnetic resonance image volumes. Med Image Comput Comput Assist Interv. 2007;10(Pt 2):402-10.
23. Zhuang X, Rhode KS, Razavi RS, Hawkes DJ, Ourselin S. A registration-based propagation framework for automatic whole heart segmentation of cardiac MRI. IEEE Trans Med Imaging. 2010 Sep;29(9):1612-25.
24. Zhuang X, Leung K, Rhode K, Razavi R, Hawkes D, Ourselin S. Whole heart segmentation of cardiac MRI using multiple path propagation strategy. Med Image Comput Comput Assist Interv. 2010;13(Pt 1):435-43.
25. Zhuang X, Yao C, Ma Y, Hawkes D, Penney G, Ourselin S. Registration-based propagation for whole heart segmentation from compounded 3D echocardiography 2010 7th IEEE International Symposium on Biomedical Imaging: From Nano to Macro, ISBI 2010 - Proceedings 2010, Article number 5490183, Pages 1093-1096.
26. Manzke R, Meyer C, Ecabert O, Peters J, Noordhoek NJ, Thiagalingam A, Reddy VY, Chan RC, Weese J. Automatic segmentation of rotational x-ray images for anatomic intra-procedural surface generation in atrial fibrillation ablation procedures. IEEE Trans Med Imaging. 2010 Feb;29(2):260-72.
27. Karim R, Mohiaddin R, and Rueckert D. Left atrium pulmonary veins: segmentation and quantification for planning atrial fibrillation ablation. Proc. SPIE 7261, 72611 T (2009)
28. Yushkevich PA, Piven J, Hazlett HC, Smith RG, Ho S, Gee JC, Gerig G. User-guided 3D active contour segmentation of anatomical structures: significantly improved efficiency and reliability. Neuroimage. 2006 Jul 1;31(3):1116-28.
29. •• Shpun S, Gepstein L, Hayam G, Ben-Haim SA. Guidance of radiofrequency endocardial ablation with real-time three-dimensional magnetic navigation system. Circulation. 1997 Sep 16;96(6):2016-21. *Early report on the CARTO EAMS.*
30. • Earley MJ, Showkathali R, Alzetani M, Kistler PM, Gupta D, Abrams DJ, Horrocks JA, Harris SJ, Sporton SC, Schilling RJ. Radiofrequency ablation of arrhythmias guided by non-fluoroscopic catheter location: a prospective randomized trial. Eur Heart J. 2006 May;27(10):1223-9. *This is a comparison of CARTO, EnSite NavX, and conventional guidance for ablation procedures.*
31. • Attili AK, Schuster A, Nagel E, Reiber JH, van der Geest RJ. Quantification in cardiac MRI: advances in image acquisition and processing. Int J Cardiovasc Imaging. 2010 Feb;26 Suppl 1:27-40. Review. *This is a detailed review of cardiac motion, perfusion, and scar imaging, and analysis.*
32. Rutz AK, Ryf S, Plein S, Boesiger P, Kozerke S. Accelerated whole-heart 3D CSPAMM for myocardial motion quantification. Magn Reson Med. 2008 Apr;59(4):755-63.
33. •• Leung KY, Bosch JG. Automated border detection in three-dimensional echocardiography: principles and promises. Eur J Echocardiogr. 2010 Mar;11(2):97-108. *Extensive review of segmentation and motion analysis techniques from 3D echo.*
34. Gebker R, Schwitter J, Fleck E, Nagel E. How we perform myocardial perfusion with cardiovascular magnetic resonance. J Cardiovasc Magn Reson. 2007;9(3):539-47.
35. Mendoza DD, Joshi SB, Weissman G, Taylor AJ, Weigold WG. Viability imaging by cardiac computed tomography. J Cardiovasc Comput Tomogr. 2010 Mar-Apr;4(2):83-91. Review.
36. Ambrose MS, Valdiviezo C, Mehra V, Lardo AC, Lima JA, George RT. CT Perfusion: Ready for Prime Time. Curr Cardiol Rep. 2010 Nov 16.
37. •• Peters DC, Wylie JV, Hauser TH, Kissinger KV, Botnar RM, Essebag V, Josephson ME, Manning WJ. Detection of pulmonary vein and left atrial scar after catheter ablation with three-dimensional navigator-gated delayed enhancement MR imaging: initial experience. Radiology. 2007 Jun;243(3):690-5. *This is a landmark paper for left atrial late enhancement MRI post–ablation treatment.*
38. Oakes RS, Badger TJ, Kholmovski EG, Akoum N, Burgon NS, Fish EN, Blauer JJ, Rao SN, DiBella EV, Segerson NM, Daccarett M, Windfelder J, McGann CJ, Parker D, MacLeod RS, Marrouche NF. Detection and quantification of left atrial structural remodeling with delayed-enhancement magnetic resonance imaging in patients with atrial fibrillation. Circulation. 2009 Apr 7;119(13):1758-67.
39. •• Knowles BR, Caulfield D, Cooklin M, Rinaldi CA, Gill J, Bostock J, Razavi R, Schaeffter T, Rhode KS. 3-D visualization of acute RF ablation lesions using MRI for the simultaneous determination of the patterns of necrosis and edema. IEEE Trans Biomed Eng. 2010 Jun;57(6):1467-75. *Validation of a novel segmentation and visualization technique for late enhancement and T2 MRI post–ablation treatment.*
40. • Dong J, Calkins H, Solomon SB, Lai S, Dalal D, Lardo AC, Brem E, Preiss A, Berger RD, Halperin H, Dickfeld T. Integrated electroanatomic mapping with three-dimensional computed tomographic images for real-time guided ablations. Circulation. 2006 Jan 17;113(2):186-94. *Early experience of CARTO-Merge validated in a dog model.*
41. Richmond L, Rajappan K, Voth E, Rangavajhala V, Earley MJ, Thomas G, Harris S, Sporton SC, Schilling RJ. Validation of computed tomography image integration into the EnSite NavX mapping system to perform catheter ablation of atrial fibrillation. J Cardiovasc Electrophysiol. 2008 Aug;19(8):821-7.
42. • Orlov MV, Ansari MM, Akrivakis ST, Jadidi A, Nijhof N, Natan SR, Wylie JV, Hicks A, Armstrong J, Jais P. First Experience with Rotational Angiogram of the Right Ventricle to Guide VT Ablation. Heart Rhythm. 2010 Oct 1. *Describes novel use of RXA for right ventricular imaging and also describes the ElectroNav electrical mapping system.*
43. Gao G, Chinchapatnam P, Wright M, Arujuna A, Ginks M, Rinaldi A, Rhode K. An MRI/CT-based cardiac electroanatomical mapping system with scattered data interpolation algorithm 7th IEEE International Symposium on Biomedical Imaging: From Nano to Macro, ISBI 2010 – Proceedings 2010, Article number 5490308, Pages 464-467.
44. • Markelj P, Tomaževič D, Likar B, Pernuš F. A review of 3D/2D registration methods for image-guided interventions. Med Image Anal. 2010 Apr 13. *This is a thorough review of 2D–3D registration for interventional applications including cardiac.*

45. Tang M, Kriatselis C, Ye G, Nedios S, Roser M, Solowjowa N, Fleck E, Gerds-Li JH. Reconstructing and registering three-dimensional rotational angiogram of left atrium during ablation of atrial fibrillation. Pacing Clin Electrophysiol. 2009 Nov;32 (11):1407-16.
46. Knecht S, Skali H, O'Neill MD, Wright M, Matsuo S, Chaudhry GM, Haffajee CI, Nault I, Gijsbers GH, Sacher F, Laurent F, Montaudon M, Corneloup O, Hocini M, Haïssaguerre M, Orlov MV, Jaïs P. Europace. Computed tomography-fluoroscopy overlay evaluation during catheter ablation of left atrial arrhythmia. 2008 Aug;10(8):931-8.
47. Duckett SG, Ginks MR, Knowles BR, Ma Y, Shetty A, Bostock J, Cooklin M, Gill JS, Carr-White GS, Razavi R, Schaeffter T, Rhode KS, Rinaldi CA. Advanced Image Fusion to Overlay Coronary Sinus Anatomy with Real-Time Fluoroscopy to Facilitate Left Ventricular Lead Implantation in CRT. Pacing Clin Electrophysiol. 2010 Oct 28.
48. Sra J, Narayan G, Krum D, Malloy A, Cooley R, Bhatia A, Dhala A, Blanck Z, Nangia V, Akhtar M. Computed tomography-fluoroscopy image integration-guided catheter ablation of atrial fibrillation. J Cardiovasc Electrophysiol. 2007 Apr;18(4):409-14.
49. Truong MVN, Aslam A, Ginks M, Rinaldi CA, Rezavi R, Penney GP, Rhode KS. 2D-3D registration of cardiac images using catheter constraints Computers in Cardiology Volume 36, 2009, Article number 5445335, Pages 605-608.
50. Rhode KS, Hill DL, Edwards PJ, Hipwell J, Rueckert D, Sanchez-Ortiz G, Hegde S, Rahunathan V, Razavi R. Registration and tracking to integrate X-ray and MR images in an XMR facility. IEEE Trans Med Imaging. 2003 Nov;22(11):1369-78.
51. •• Rhode KS, Sermesant M, Brogan D, Hegde S, Hipwell J, Lambiase P, Rosenthal E, Bucknall C, Qureshi SA, Gill JS, Razavi R, Hill DL. A system for real-time XMR guided cardiovascular intervention. IEEE Trans Med Imaging. 2005 Nov;24(11):1428-40. *This paper describes MR to X-ray image fusion for XMR systems and several EP applications.*
52. King AP, Rhode KS, Ma Y, Yao C, Jansen C, Razavi R, Penney GP. Registering preprocedure volumetric images with intraprocedure 3-D ultrasound using an ultrasound imaging model. IEEE Trans Med Imaging. 2010 Mar;29(3):924-37.
53. Ma YL, Penney GP, Rinaldi CA, Cooklin M, Razavi R, Rhode KS. Echocardiography to magnetic resonance image registration for use in image-guided cardiac catheterization procedures. Phys Med Biol. 2009 Aug 21;54(16):5039-55.
54. Ma Y, Penney GP, Bos D, Frissen P, Rinaldi CA, Razavi R, Rhode KS. Hybrid echo and x-ray image guidance for cardiac catheterization procedures by using a robotic arm: a feasibility study. Phys Med Biol. 2010 Jul 7;55(13):N371-82.
55. Gao G, Penney GP, Gogin N, Cathier P, Arujuna A, Wright M, Caulfield D, Rinaldi CA, Razavi R, Rhode KS. Rapid image registration of three-dimensional transesophageal echocardiography and x-ray fluoroscopy for the guidance of cardiac interventions Information Processing in Computer-Assisted Interventions, First International Conference, IPCAI 2010, Geneva, Switzerland, June 23, 2010. Proceedings. Lecture Notes in Computer Science 6135 Springer 123-134 2010.
56. •• D. Noble, "A modification of the Hodgkin–Huxley equations applicable to purkinje fibre action and pace-maker potentials," J Physiol, vol. 160, pp. 317–352, 1962. *Seminal paper on cardiac electrophysiology modeling.*
57. C. Luo and Y. Rudy, "A model of the ventricular cardiac action potential: depolarization, repolarization, and their interaction," Circulation Research, vol. 68, pp. 1501–1526, 1991.
58. K. Ten Tusscher, D. Noble, P. Noble, and A. Panfilov, "A model of the human ventricular myocyte," American Journal of Physiology - Heart and Circulatory Physiology, vol. 286, no. 4, pp. 1573–1589, 2004.
59. • A. Garny, D. Noble, and P. Kohl, "Dimensionality in cardiac modelling," Prog Biophys Mol Biol, vol. 87, no. 1, pp. 47–66, Jan 2005. *Clearly explains the computing challenge in simulations at the organ scale.*
60. M. Fink and D. Noble, "Markov models for ion channels: versatility versus identifiability and speed," Philosophical Transactions of the Royal Society A: Mathematical, Physical and Engineering Sciences, vol. 367, no. 1896, p. 2161, 2009.
61. A. Panfilov and J. Keener, "Re-entry in an anatomical model of the heart," Chaos, Solitons & Fractals, vol. 5, no. 3-4, pp. 681–689, 1995.
62. J. Jalife and R. Gray, "Drifting vortices of electrical waves underlie ventricular fibrillation in the rabbit heart," Acta Physiologica Scandinavica, vol. 157, no. 2, pp. 123–132, 1996.
63. E. Cherry and F. Fenton, "Suppression of alternans and conduction blocks despite steep APD restitution: electrotonic, memory, and conduction velocity restitution effects," American Journal of Physiology- Heart and Circulatory Physiology, vol. 286, no. 6, p. H2332, 2004.
64. C. Clancy and Y. Rudy, "Linking a genetic defect to its cellular phenotype in a cardiac arrhythmia," Biol, vol. 9, pp. 295–305, 1995.
65. N. Trayanova and B. Tice, "Integrative computational models of cardiac arrhythmias-simulating the structurally realistic heart," Drug Discovery Today: Disease Models, 2009.
66. M. Killeen, I. Sabir, A. Grace, and C. Huang, "Dispersions of repolarization and ventricular arrhythmogenesis: Lessons from animal models," Progress in biophysics and molecular biology, vol. 98, no. 2-3, pp. 219–229, 2008.
67. A. Yue, M. Franz, P. Roberts, and J.Morgan, "Global endocardial electrical restitution in human right and left ventricles determined by noncontact mapping," Journal of the American College of Cardiology, vol. 46, no. 6, p. 1067, 2005.
68. H. Arevalo, B. Rodriguez, and N. Trayanova, "Arrhythmogenesis in the heart: Multiscale modeling of the effects of defibrillation shocks and the role of electrophysiological heterogeneity," Chaos: An Interdisciplinary Journal of Nonlinear Science, vol. 17, p. 015103, 2007.
69. I. Banville and R. Gray, "Effect of action potential duration and conduction velocity restitution and their spatial dispersion on alternans and the stability of arrhythmias," Journal of cardiovascular electrophysiology, vol. 13, no. 11, pp. 1141–1149, 2002.
70. M. Nash, C. Bradley, P. Sutton, R. Clayton, P. Kallis, M. Hayward, D. Paterson, and P. Taggart, "Whole heart action potential duration restitution properties in cardiac patients: a combined clinical and modelling study," Experimental physiology, vol. 91, no. 2, p. 339, 2006.
71. R. C. Kerckhoffs, J. Lumens, K. Vernooy, J. H. Omens, L. J. Mulligan, T. Delhaas, T. Arts, A. D. McCulloch, and F. W. Prinzen, "Cardiac resynchronization: Insight from experimental and computational models," Prog Biophys Mol Biol, vol. 97, no. 2-3, pp. 543–561, Jun-Jul 2008.
72. R. C. Kerckhoffs, A. D. McCulloch, J. H. Omens, and L. J. Mulligan, "Effects of biventricular pacing and scar size in a computational model of the failing heart with left bundle branch block," Med Image Anal, Jul 2008.
73. M. Sermesant, J. M. Peyrat, P. Chinchapatnam, F. Billet, T. Mansi, K. Rhode, H. Delingette, R. Razavi, and N. Ayache, "Toward patient-specific myocardial models of the heart," Heart Failure Clinics, vol. 4, no. 3, pp. 289–301, July 2008.
74. • R. C. P. Kerckhoffs, Ed., Patient-Specific Modeling of the Cardiovascular System, Technology-Driven Personalized Medicine. Springer, 2010. *Reviews different projects in cardiac model personalization.*
75. J.-M. Peyrat, M. Sermesant, X. Pennec, H. Delingette, C. Xu, E. R. McVeigh, and N. Ayache. A Computational Framework for the Statistical Analysis of Cardiac Diffusion Tensors: Application to a

Small Database of Canine Hearts. *IEEE Transactions on Medical Imaging*, 26(11):1500-1514, November 2007

76. N. Toussaint, C. T. Stoeck, S. Kozerke, M. Sermesant, and P. G. Batchelor. In-vivo Human 3D Cardiac Fibre Architecture: Reconstruction Using Curvilinear Interpolation of Diffusion Tensor Images. In *Proc. Medical Image Computing and Computer Assisted Intervention (MICCAI'10)*, LNCS, Beijing, China, September 2010. Springer.
77. J. Relan, P. Chinchapatnam, M. Sermesant, K. Rhode, H. Delingette, R. Razavi, and N. Ayache, "Coupled personalisation of electrophysiology models for simulation of induced ischemic ventricular tachycardia," in Medical Image Computing and Computer-Assisted Intervention–MICCAI 2010, ser. Lecture Notes in Computer Science (LNCS), vol. 6362. Springer, 2010, pp. 420–428.
78. M. Sermesant, F. Billet, R. Chabiniok, T. Mansi, P. Chinchapatnam, P. Moireau, J.-M. Peyrat, K. Rhode, M. Ginks, P. Lambiase, S. Arridge, H. Delingette, M. Sorine, A. Rinaldi, D. Chapelle, R. Razavi, and N. Ayache, "Personalised electromechanical model of the heart for the prediction of the acute effects of cardiac resynchronisation therapy," in Proceedings of Functional Imaging and Modeling of the Heart 2009 (FIMH'09), ser. LNCS, vol. 5528. Springer, 3-5 June 2009, pp. 239–248.